Mobile ionic impurities in organic semiconductors

Rep, D.B.A.; Morpurgo, Alberto; Sloof, W. G.; Klapwijk, T. M.

Mobile ionic impurities in organic semiconductors

Cite as: Journal of Applied Physics **93**, 2082 (2003); https://doi.org/10.1063/1.1538338
Submitted: 25 September 2002 • Accepted: 25 November 2002 • Published Online: 30 January 2003

D.B.A. Rep, A. F. Morpurgo, W. G. Sloof, et al.

Mobile ionic impurities in organic semiconductors

D.B.A. Rep and A. F. Morpurgo[a)]
Faculty of Applied Sciences, Department of NanoScience, Delft University of Technology, Lorentzweg 1, 2628 CJ Delft, The Netherlands

W. G. Sloof
Faculty of Applied Sciences, Laboratory of Materials Science, Delft University of Technology, Rotterdamseweg 137, 2628 AL Delft, The Netherlands

T. M. Klapwijk
Faculty of Applied Sciences, Department of NanoScience, Delft University of Technology, Lorentzweg 1, 2628 CJ Delft, The Netherlands

(Received 25 September 2002; accepted 25 November 2002)

We study the stability in time of the current–voltage characteristics of organic thin-film devices on glass substrates. We find for poly(3-hexylthiophene) and for pentacene that the resistance of the devices gradually changes under the application of an electrical bias depending on the sodium content of the glass substrates used in the experiment. For devices on a very common type of glass (with a Na_2O content of about 6%) and on sodalime glass (14% Na_2O) substrates, the prolonged application of a voltage bias results in a substantial decrease (up to two orders of magnitude) of the bulk and contact resistances, whereas for sodium-free glass substrates the gradual changes in current–voltage characteristics are much smaller. A systematic study of the electrical behavior complemented by chemical analysis shows that the instabilities observed are due to Na^+ ions diffusing from the substrate into the organic film, and moving inside the organic material as a result of the applied electric field. Our results show in detail how ion motion in organic materials results in substantial hysteresis and device instabilities. © *2003 American Institute of Physics.*
[DOI: 10.1063/1.1538338]

I. INTRODUCTION

Over the past few years, there has been continuous progress in improving the properties of organic semiconducting materials to such an extent that they can be implemented into electronic devices for practical applications.[1] However, the study and optimization of such devices is often hampered by material and device instabilities during operation. Well-known examples of instabilities are provided by hysteresis and voltage shifts in the current versus gate-voltage characteristics of organic thin-film transistors,[2–7] or by the degradation of organic light-emitting diodes during device operation.[8,9] Such time-dependent changes in the electrical properties can gravely affect device performance, especially when they are irreversible and eventually lead to device failure. In addition, they cause severe problems in the study of charge transport in organic semiconducting devices, since time-dependent changes can easily lead to misinterpretations of the current–voltage ($I-V$) characteristics.

Instabilities in the properties of organic semiconductors are not often discussed in literature. Either the time dependence of the electrical characteristics is not investigated, or materials which display gradual changes in their properties are replaced in device applications by more stable materials. This is done for practical reasons but has as a result that little is known about the physical origin of electrical instabilities despite their importance for applications and fundamental studies. Several physical mechanisms have been proposed to account for time-dependent effects, such as trapping of charges,[2] impurity motion,[5,6] or the chemical degradation of the organic material.[8] Although plausible, these proposed mechanisms are not normally substantiated by a systematic analysis of the time-dependent effects or other evidence to conclusively identify the origin of the effects.

The present work deals with one specific case of electrical instabilities in organic devices, namely instabilities in the $I-V$ characteristics of organic thin films on glass substrates. Specifically, we have prepared thin films of a polymeric and small-molecule conjugated material on different types of glass substrates and observed large and reversible changes in the metal/organic/metal device resistance during the application of an electrical field. Chemical analysis indicates that the changes are accompanied by the diffusion of positively charged sodium ions from the glass substrate and into the organic material. We demonstrate that the electric-field-driven redistribution of ionic impurities systematically causes hysteresis effects and device instabilities during operation of organic thin-film devices.

The similarity of results obtained on solution-processed polymer films and vacuum-evaporated small-molecule films indicates that ion motion affects a wide range of organic materials in a similar way. Furthermore, our results demonstrate that the choice of substrate is crucial for device applications as well as for fundamental studies of charge transport in organic semiconductors. It is worth stressing that, in literature studies of electronic transport in organic semiconduc-

a)Electronic mail: a.morpurgo@tnw.tudelft.nl

tors, similar glass substrates are used frequently but the glass specifications are usually omitted.

II. EXPERIMENTAL PROCEDURES

A. Devices and materials

Glass substrates with predefined electrodes were used. The glass specifications are listed in the text. Samples were briefly washed with polar and nonpolar solvents before application of the organic layers. The device geometry consists of interdigitated electrodes (see inset of Fig. 6) with interelectrode separations L ranging from 1 to 20 μm and effective electrode widths W ranging from 1 to 50 cm.

We use two widely studied examples of organic conjugated materials: Pentacene (as an example of small-molecule organic semiconductors), and poly(3-hexylthiophene) (P3HT) (as an example of polymeric semiconductors). Both materials have received much attention because of their high charge-carrier mobility (up to 0.1 $cm^2/V\,s$ for P3HT[10] and 1.5 cm^2/Vs for pentacene,[11] and are employed in many studies of organic devices such as thin-film field-effect transistors. Thin films of P3HT were prepared by spincoating the polymer from a 1 wt % chloroform solution on glass substrates with prepatterned Au electrodes. The electrodes were defined using standard lithographic techniques. Regioregular P3HT was obtained from Philips Research Laboratories, The Netherlands, where it was synthesized as described elsewhere.[12] Thin films of pentacene were prepared by vacuum evaporation onto substrates kept at room temperature. Pentacene (Aldrich, 98%) was used as received.

To evaluate the electrical properties of the films on glass, the devices were introduced in a cryostat system (10^{-7} to 10^{-6} mbar). As prepared, the pentacene films are undoped, whereas P3HT is doped by exposure to the ambient atmosphere during preparation. This is due to oxygen diffusion into the P3HT, as has been established in literature.[13,14] Before performing measurements, we reduced the oxygen dopant concentration of P3HT substantially, by briefly heating the devices *in vacuo* up to temperatures between 425 and 440 K.[13] This lowers the overall doping level of the P3HT, owing to the outdiffusion of oxygen. Reducing the doping level prevents current-induced heating of the P3HT film during current flow which also causes dedoping and affects the $I-V$ characteristics in a time-dependent way. All electrical measurements were performed using a Keithley 4200 semiconductor characterization system.

B. X-ray photoelectron spectroscopy

Spectra of the Na 1*s*, C 1*s*, S 2*p*, O 1*s*, Si 2*p*, and Au 4*f* photoelectron lines and the Na $KL_{23}L_{23}$ Auger line were recorded with a PHI 5400 ESCA instrument set at a constant analyzer pass energy of 44.75 eV and with a step size of 0.2 eV, using unmonochromatized incident Al x-ray radiation ($\mathrm{Al}\,K\alpha_{1,2}=1486.6\,\mathrm{eV}$). The energy scale of the spherical capacitor analyzer spectrometer was calibrated according to the procedure described in Ref. 15. The electrons emitted from the specimen were detected at an angle of 45° with respect to the specimen surface. An elliptic area of 0.6 $\times 0.8$ mm of the sample surface was analyzed. For the determination of composition depth profiles, alternate sputtering and spectra acquisition was employed. Toward this end, a 4 keV Ar^+ beam was used at 40° to the specimen surface normal. During sputtering, the ion beam was scanned over an area of 5×5 mm on the specimen surface. In this case, spectra were recorded with an analyzer pass energy of 89.45 eV and a step size of 0.5 eV. The composition was determined from the area of the photoelectron lines after background subtraction adopting elemental sensitivity factors.[16]

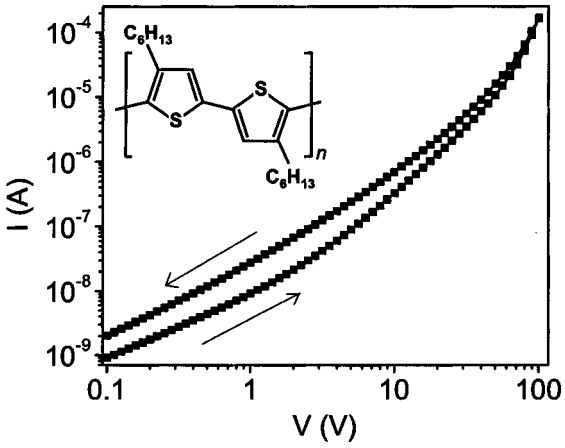

FIG. 1. Typical $I-V$ characteristics of a Au/P3HT/Au device on Schott D263 borosilicate glass. The voltage is swept up and back down, as indicated by the arrows. The currents during the sweep up are lower than during the sweep down. Very similar hysteresis is observed in all samples investigated. Total electrode width $W=1$ cm; interelectrode separation $L=10$ μm. The structure formula of P3HT is shown as an inset.

III. RESULTS

In the following, we present measurements of time-dependent changes in the electrical characteristics of P3HT and pentacene films on glass. The results we discuss are typical examples of measurements performed on a large number of samples exhibiting systematic and reproducible behavior. The experimental results are organized in the following manner. First, we investigate P3HT devices prepared on a very common type of glass (see Sec. III A). As we have determined that hysteresis effects are sensitive to the choice of glass substrate, we compare different types of glass in Sec. III B. Measurements are also done for the case of pentacene (Sec. III C). In Sec. III D, we investigate the nature of the impurities in the organic material. We end with a discussion of our observations and with our conclusions.

A. Hysteresis effects in P3HT devices on glass

Figure 1 shows the room-temperature $I-V$ characteristics of a Au/P3HT/Au device on very common borosilicate-type glass (Schott D263). The characteristics are linear for low bias and nonlinear for higher bias. When measurements are performed up to a higher bias, hysteresis systematically appears in the $I-V$ curves. Hysteresis is manifested by a difference in current during the voltage sweep up compared to the subsequent sweep back down.

The magnitude of hysteresis is found to depend on the sweeping speed and on the voltage range used in the mea-

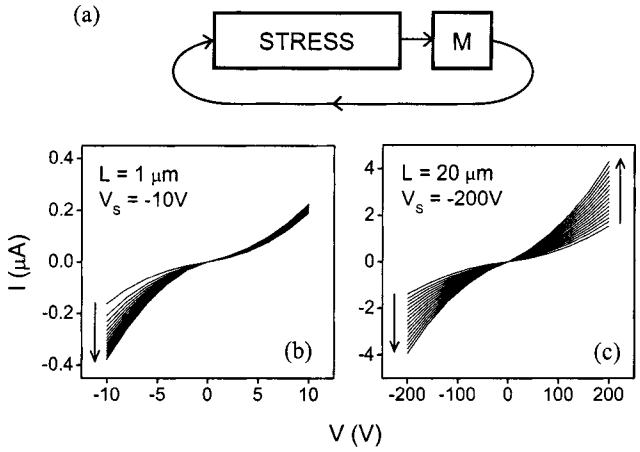

FIG. 2. (a) Schematic representation of the stress measurement cycles. Each cycle consists of a long period of continuous stressing at voltage V_S ("STRESS") followed by a fast measurement ("M") of an $I-V$ curve. Bottom panels: $I-V$ curves measured in between subsequent stress periods of 120 s at stress voltage V_S. The left-hand side panel is for an interelectrode separation of 1 μm and shows the emergence of asymmetry in the $I-V$ characteristics during electrical stress. The right-hand side panel is for a separation of 20 μm, revealing a nearly symmetric increase in current. The change in current with stressing time is indicated by the arrows. Devices were prepared on plain glass with a total electrode width of 1 cm.

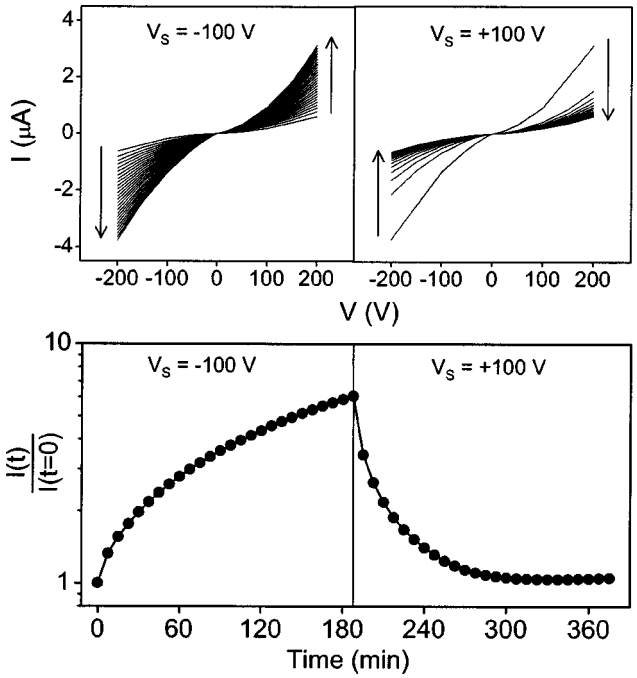

FIG. 3. Upper panels: $I-V$ characteristics of a P3HT device ($L=10$ μm and $W=1$ cm) on plain glass, measured in between 25 subsequent stress periods of 450 s at $V_S=-100$ V (left-hand side upper panel) followed by 25 stress periods at $V_S=+100$ V (right-hand side upper panel). A nearly symmetric increase in current is observed during the first stress sequence, which is reversed by reversing the stress polarity. The lower panel shows the change in current measured at $V=100$ V as a function of stressing time, determined from the $I-V$ curves of the upper panels.

surements. Its counterclockwise direction indicates that the current increases with time under the influence of the applied voltage. The current increase can reach an order of magnitude during a single sweep. This is a very significant effect which cannot be ignored when studying the device characteristics.

To investigate the hysteresis behavior in more detail, we stressed devices electrically by applying a constant stress voltage V_S, interrupting at regular intervals to measure an $I-V$ curve. Figure 2 shows two typical examples of the stress-induced changes in the Au/P3HT/Au device characteristics. The data shown in Fig. 2 confirm that the current through the device increases with time under the influence of a stress voltage. For interelectrode separations L larger than about 5 μm, the increase is similar for both positive and negative measurement voltages [Fig. 2(c)], while smaller separations display an increase in the current mostly in one voltage polarity [Fig. 2(b)]. This results in asymmetric $I-V$ characteristics as opposed to symmetric characteristics for longer separations.

We have investigated the dependence of the current changes on the magnitude and sign of the stress voltage and found that the current returns to its original value after removing the stress bias or reversing the stress bias polarity (Fig. 3). By maintaining the opposite sign of the stress voltage for even longer periods of time, the current can be seen to increase again. For devices with a small interelectrode separation, the increase after reversing the stress bias is observed for the voltage polarity *opposite* to that of the original increase. This observation shows that the mechanism responsible for the current increase is sensitive to the polarity of the stress voltage. Specifically, the asymmetry in small devices is systematically such that we measure a much larger current when the measurement voltage V has the same polarity as the stress voltage V_S. Finally, the current increase with time is accelerated by increasing the stress voltage magnitude or by increasing the temperature (not shown).

The observed increase in current obviously corresponds to a decrease of the device resistance. In general, the resistance of a metal/polymer/metal device is determined by the metal/polymer contact resistances and by the "bulk" resistance of the film, the latter increasing with increasing L. The distinct difference between stress effects observed in short devices ($L\lesssim 5$ μm) and long devices ($L\gtrsim 5$ μm) shown in Fig. 2 allows us to discriminate between contact and bulk effects. In short devices, the appearance of a large asymmetry after stressing indicates that contact resistances dominate the electrical characteristics: It is this contact resistance which changes during stressing. The presence of a contact resistance at the Au/P3HT interface is consistent with observations discussed elsewhere.[17,18] On the other hand, the *symmetric* characteristics we observe, while stressing long devices, demonstrate that also the bulk resistance of the P3HT film decreases during the application of electrical stress.

To further investigate the origin of the current increase, we have measured the $I-V$ characteristics as a function of temperature. Figure 4(a) shows that the conductivity of a device with $L=20$ μm (the bulk-dominated conductivity) is thermally activated, $\sigma=\sigma_0\exp(-E_{\mathrm{act}}/k_BT)$, with k_B representing Boltzmann's constant, T the temperature, and E_{act} the activation energy. The data demonstrate that a large decrease in activation energy occurs upon stressing the device. For short ($L<5$ μm) devices with asymmetric characteris-

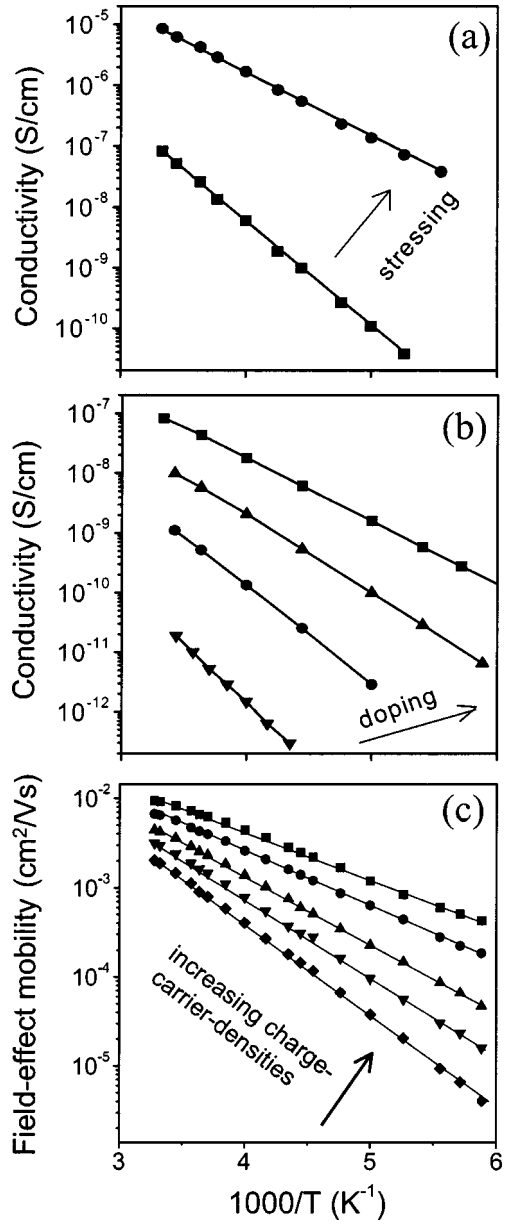

FIG. 4. (a) Conductivity (measured at $V=1$ V) of a 20 μm P3HT device as a function of temperature, before and after stressing overnight at $V_S=200$ V. (b) Ohmic conductivity of a P3HT thin film for increasing doping levels (as reported in Ref. 13). The increase in carrier density was achieved by exposing the film to air. (c) Field-effect mobility of charge carriers in P3HT for increasingly large values of the gate voltages (see Ref. 13). Note the similar change in activation energy induced by stressing and by an increase in carrier density due to chemical doping or electrostatic accumulation of charges.

tics, the conductivity was also found to be thermally activated and it was observed that the activation energy depends on the direction of current flow (i.e., on the measurement-voltage polarity).

The change in activation energy of the bulk conductivity with stressing strongly resembles the effect of changing the overall carrier density of the P3HT, either by chemical doping or by electrostatic accumulation of charges.[13] A comparison between the three situations is shown in Fig. 4. The change in asymmetry of the device characteristics can also be related to a change in local doping level: We and others have found that the Au/P3HT contact resistance is sensitive to the local doping level.[17,18] Thus, we conclude that electrical stress changes the $I-V$ characteristics of P3HT devices on glass in a very similar way to an increase in the free carrier density.

TABLE I. Composition (in wt %) of the three types of glass substrates used in this work: Schott AF45 borosilicate glass (alkali free), Schott D263 borosilicate glass (plain), and soda-lime glass (alkali rich)

Glass	SiO_2	Al_2O_3	Na_2O	B_2O_3	BaO
Alkali-free	50	11	<0.02	14	24
Plain	64	4	6	8	<1
Alkali-rich	71	2	14	<1	<1

B. P3HT on alkali-rich and alkali-free glass

In the course of our experiments, we have observed that the behavior of the electrical instabilities in time correlates to the specific kind of glass substrate used. The difference between glass substrates is mainly in their alkali content. For example, the glass substrates discussed in Sec. III A have a concentration of about 8% Na_2O while alternative types of glass, such as Schott AF45 borosilicate glass and soda-lime glass, have significantly different concentrations of Na_2O. In this section. we therefore compare the response to stress of P3HT devices prepared under nominally identical conditions on different kinds of glass substrates containing either a high alkali content, low alkali content or an intermediate alkali content (see Table I).

The response to electrical stress of devices prepared on alkali-rich and alkali-free glass is shown in Fig. 5 for the case of P3HT. The preparation and thermal dedoping procedures were the same for all types of devices. After dedoping, the low-field linear conductivities of all devices were comparable. The response of the two types of devices to high electric fields as a function of time, however, is very different. It can be seen in Fig. 5 that the stress-induced changes are much stronger for the case of alkali-rich glass. This demonstrates the crucial role of the glass substrate for the stability of the device conductivity during stressing. The measurements performed on ''plain'' glass discussed in Sec. III A were found to be the intermediate situation of the alkali-free and alkali-rich behavior in that the changes with time during similar stress were larger than those shown for alkali-free glass but smaller than alkali-rich glass.

Remarkably, the *direction* of current asymmetry which emerges during stressing of a P3HT film on alkali-rich (or plain) glass is opposite to that of P3HT on alkali-free glass. In the former case, the current is largest in the stress-bias direction, while in the latter case; the current is largest in the direction *against* the stress-bias direction. In addition, the current changes are orders-of-magnitude smaller for films prepared on alkali-free glass.

After several minutes of continuous stressing a P3HT/alkali-rich device at one voltage polarity, white spots appear on the fingers of the cathode (the electrode with the lowest potential). This is shown in Fig. 6. After even longer periods of electrical stress, the alkali-rich samples break down, as

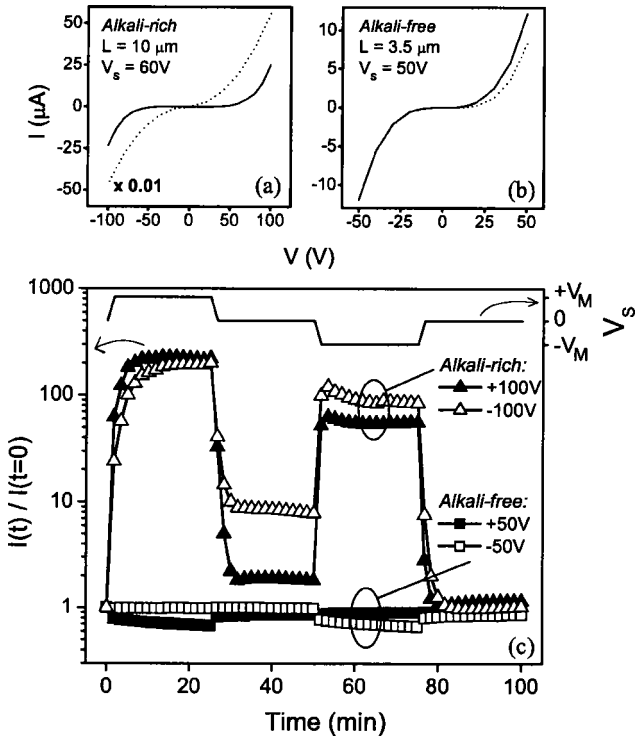

FIG. 5. Response to electrical stress of dedoped P3HT devices prepared on alkali-rich glass and alkali-free glass. The sensitivity to the magnitude and polarity of the stress bias was investigated by stressing at four values of V_S ($+V_M$, 0, $-V_M$, and 0) as indicated in the upper curve in panel (c). Panels (a) and (b) show the $I-V$ curves measured before (solid line) and after (dotted line) the first 25 min stress at $+V_M$. Notice that after stress, the current through the device on alkali-rich glass has increased by orders of magnitude while that of the device on alkali-free glass has decreased slightly. For all types of glass, the changes are sensitive to the stress-bias polarity, causing asymmetry in the $I-V$ characteristics. The device geometries and stress voltage magnitudes were as follows. Alkali-rich glass: $L=10\ \mu$m, $W=50$ cm, and $V_M=60$ V. Alkali-free glass: $L=3.5\ \mu$m, $W=50$ cm, and $V_M=50$V.

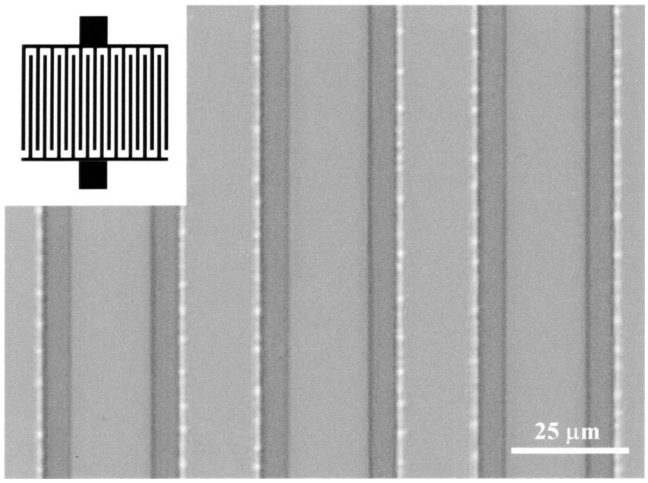

FIG. 6. Optical microscope image of a P3HT device prepared on Na-rich glass after several hours of continuous stressing. The image reveals visible material degradation near the electrode which was kept on negative voltage (cathode) during application of the stress bias. The degradation shows up as bright-colored areas. Inset: Schematic picture of the interdigitated electrode structure (top view, not to scale).

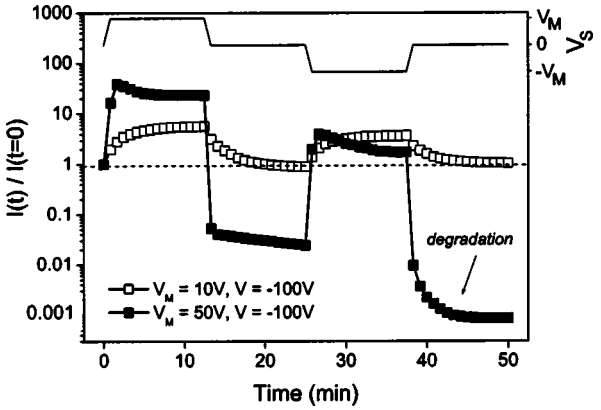

FIG. 7. Response to electrical stress of a P3HT device ($L=10\ \mu$m) prepared on alkali-rich glass for two subsequent sequences of stress. Each stress sequence consist of four values of V_S ($+V_M$, 0, $-V_M$, and 0) as indicated in the top part of the graph. In the first sequence ($V_M=10$ V), the changes are typical examples of reversible stress effects, but the second sequence, which has a larger stress bias ($V_M=50$ V), shows irreversible degradation of the device characteristics. The irreversible degradation is accompanied by optically visible degradation of the material near the cathode (see Fig. 6).

borne out by a sudden and irreversible drop in the current (Fig. 7). The white spots and the degradation effects are absent on plain or alkali-free glass samples after similar periods of electrical stress. This suggests that electrical breakdown is related to the visible change in material properties of the P3HT near the cathode.

C. Pentacene on alkali-rich and alkali-free glass

The response to stress of pentacene devices on alkali-rich and alkali-free glass is shown in Fig. 8. As in the case of P3HT devices, the stress-induced changes in the electrical properties of devices on alkali-rich glass are much larger than those on alkali-free glass. The asymmetry that emerges after the application of a stress bias on alkali-rich substrates is stronger than that of similar P3HT devices, with the current in the same voltage polarity as the stress bias increasing

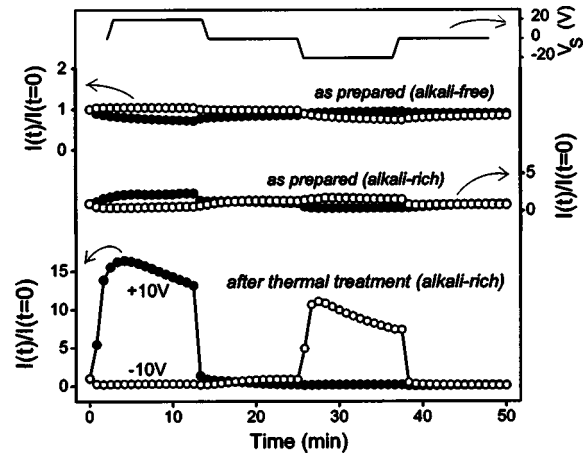

FIG. 8. Response to electrical stress of pentacene devices ($L=10\ \mu$m) prepared on alkali-rich glass and alkali-free glass, before and after a thermal treatment (in situ) of 20 min at 400 K. The stress voltages are in the upper trace. The measurement voltages are $+10$ V (filled symbols) and -10 V (open symbols). Note that the response to electrical stress is substantially enhanced by the thermal treatment.

TABLE II. Atomic sodium concentration and number of sodium atoms per sulphur atom in the P3HT layer on alkali-rich or alkali-free glass, as identified by XPS. (1): Outside the electrode area; (2): Directly over the electrode area. From these measurements, we conclude that the sodium concentration in dedoped P3HT on alkali-rich glass substrates is at least one order of magnitude higher than on alkali-free substrates

Glass	P3HT	[Na]	[Na]/[S]
Alkali-rich	as-prepared	<0.1	
Alkali-rich	dedoped (1)	0.7–1.1	0.15–0.25
Alkali-rich	dedoped (2)	0.9-2.5	0.2–0.4
Alkali-free	dedoped	<0.1	

and the current in the opposite polarity decreasing during stress. This results in an asymmetry factor $I(V=+10\,\mathrm{V})/I(V=-10\,\mathrm{V})$ of about 100 when $V_S=+20\,\mathrm{V}$.

It is worth noting that such a large effect is only produced by a stress voltage *after* a thermal treatment. For devices prepared on alkali-rich glass that were not subjected to a thermal treatment, the electrical stress effects are much smaller, as can be seen in Fig. 8. In comparing this to the case of P3HT, we remark that a thermal treatment preceding the measurements on P3HT cannot be avoided in order to remove most of the oxygen-related dopants. If not removed, these dopants cause a high current level and, therefore, considerable Joule heating. The Joule heating and the vacuum environment in which the measurements are performed results in dedoping of the polymer film.[13,19] The Joule-heating-induced dedoping causes a time-dependent change in the electrical characteristics of the film which obscures the effects under investigation.

Finally, we have determined that the pentacene devices on alkali-rich glass do not break down in a similar fashion to the P3HT devices on alkali-rich substrates. The white coloring of the cathode after long periods of stress is absent when stressing pentacene instead of P3HT.

D. X-ray photoelectron spectroscopy analysis

To investigate the contamination of the organic film prepared on alkali-rich glass, we have performed an elements analysis of a typical P3HT device by means of x-ray photoelectron spectroscopy (XPS). Table II shows the XPS results of P3HT films on different types of glass, after various treatments. Significant sodium contamination of the P3HT film appears after thermal treatment of devices prepared on alkali-rich glass. In the case of alkali-rich glass without thermal treatment and electrical stress, or devices prepared on alkali-free glass, contamination is below the detection limit of the XPS apparatus. This shows that sodium diffuses during the thermal treatment from the substrate into the polymer film.

With the sulphur atomic concentration [S] as a measure of the concentration of thiophene rings, the XPS results listed in Table II reveal an average contamination of about 1 sodium per 5 thiophene rings of the P3HT. This corresponds to a concentration of about $8\times10^{20}\,\mathrm{cm}^{-3}$. [20] Comparing XPS data taken on different regions on an actual device, we find that the average Na concentration in the region of the

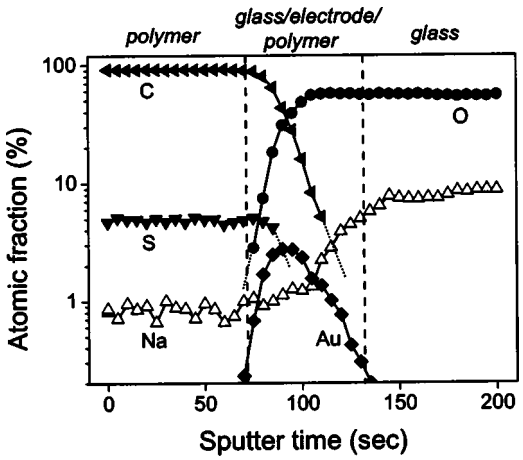

FIG. 9. Relative amounts of the dominant elements identified by XPS for a P3HT device on alkali-rich glass with Au electrodes. The device has interdigitated gold electrodes (as opposed to a full gold layer in between glass and polymer) so that there is a region in which the elements from the electrodes, the polymer and the glass are seen at the same time. Elements: oxygen (●), sodium (Δ), sulphur (▼), gold (♦) and carbon (◀). Dotted lines indicate that the signal falls below the detection limit of the experiment. This measurement demonstrates a uniform distribution of sodium in the organic material on alkali-rich glass.

electrodes of a stressed device on alkali-rich glass is slightly higher (by a factor of 2, at the most) than in regions away from the electrode area (see Table II).

We have determined a depth profile of the sodium contamination by sputtering slowly through the device, and well into the substrate, interrupting every few minutes to perform XPS analysis (Fig. 9). The depth profile clearly reveals the polymer,[21] the glass, and an intermediate region near the Au electrodes. It also reveals a uniform distribution of sodium throughout the polymer thickness.

Finally, we have investigated the nature of the sodium impurities by determining the position of the $\mathrm{Na}\,KL_{23}L_{23}$ Auger line. The sum of this energy and that of the Na 1*s* photoelectron line is known as the Auger parameter (AP). It is an important indication of the chemical nature of an element.[22] We find $\mathrm{AP_{Na}}=(2063.8\pm0.3)\,\mathrm{eV}$. This value is significantly higher than reported Auger parameters of sodium compounds such as Na_2O (2062.3 eV) or Na_2SO_3 (2061.7 eV) but lower than that of pure Na (2066 eV).[23] We infer from this analysis that a large fraction of the sodium is dispersed as Na^+ inside the polymer material. Because the electrostatic screening of atomic sodium dispersed in the organic medium is different from that in pure sodium, the AP is lower than 2066 eV. This environmental lowering of the AP is a well-known phenomenon. It has been observed, for example, when comparing a pure solid and a gas (i.e., free atoms dispersed in air).[22] The possibility of atomic sodium (Na) instead of Na^+ can be discarded because of the high reactivity of this atom.

It is important to note the visible contamination of P3HT devices near the electrodes at which Na^+ is accumulated (Fig. 6) suggests a chemical reaction. The absence of visible contamination in devices with pentacene further indicates that the reaction is specific to the thiophene ring of the P3HT. Our XPS measurements do not indicate the formation of a

known sodium compound. This might be due to the fact that the contamination is localized in a narrow region near the cathode so that the total amount averaged over the entire XPS analysis window ($0.6\times0.8\,mm^2$) might be too low for detection. Alternatively, a sodium compound might be formed whose AP has not yet been determined and tabulated.

IV. DISCUSSION

The analysis of the experimental results discussed so far allows us to draw specific conclusions as to the origin of the electrical instabilities observed. In particular, we can demonstrate that the instabilities are due to the Na^+ ions which diffuse from the glass substrate into the organic film. When an electric field is applied, the ions redistribute, thus causing a change in the electrostatic profile inside the film. This affects the measured transport properties. We will argue that, when the negative counter ions of the sodium are taken into account, the net effect of the ionic redistribution in the film is qualitatively very similar to that of an electrostatic gate in a field-effect transistor, or a change in carrier density by means of (de)doping.

A. Sodium impurity diffusion and redistribution

The comparison of the electrical behavior of organic films prepared on different kinds of glass substrates (Figs. 5 and 8) clearly indicates that the electrical instabilities observed in these films are related to the presence of sodium compounds in the glass. In particular, the instabilities are much more pronounced for films prepared on substrates with a larger sodium content.

More specifically, our measurements indicate that the instabilities are cuased by sodium impurities that have diffused from the glass into the organic film, while the device is kept at an elevated temperature. This follows from the XPS analysis of devices on the different types of glass substrates (Table II) and from the electrical behavior of pentacene films observed before and after heating to 400 K (Fig. 8). The dependence on temperature of the amount of sodium contamination inside the organic film is consistent with the fact that impurity diffusion in solids is normally a thermally activated process.[24]

We note at this point that Na^+ diffusion from glass substrates is well known, especially for the case of alkali-rich glass.[24] Sodium ions can migrate even through silicon dioxide films and affect layers deposited on top of these oxides. For example, Na^+ ions migrating into a Si layer in metal–oxide–semiconductor field-effect transistors are known to cause unwanted threshold voltage shifts.[25] The motion and presence of counterions, to ensure charge neutrality, has not been identified conclusively. Experimental evidence has been presented suggesting that protons (H^+) move in the opposite direction of the sodium ion motion and thus ensure charge neutrality. Motion of negatively charged ions, i.e., O^{2-} ions in the case of oxidic glasses, is unlikely because of the low diffusion constant of O^{2-}. [24]

Analysis of our XPS measurements (Sec. III D) indicates that most of the sodium inside the organic film is not involved in a strong ionic bond but rather that it is Na^+. The observation of visible contamination of the P3HT near the cathode (the negative electrode) after long stressing times (Fig. 6) confirms the ionic nature of the sodium. Positive ions will move inside the organic film toward the cathode under the influence of the applied electric field. Finally, the ionic nature of the sodium is in correspondence with the sensitivity of the electrical instabilities to the polarity of the stress voltage. The electric-field induced accumulation of sodium ions results in very high local concentrations of sodium near the cathode which might give rise to some chemical reaction and thus visible damage.

The transport measurements provide additional information about the effect of Na^+ on the electrical characteristics of the organic films. Specifically, we can conclude that the ions do not *dope* the organic semiconductor. This we conclude because the low-field linear $I-V$ characteristics of film deposited on sodium-rich glass is not significantly higher after dedoping than similar films on sodium-free glass. Only after the application of a stress bias do the devices on different types of glass display very different electrical behaviors. This conclusion is in line with a previous studies of thiophene-based materials including P3HT.[26,27] In these studies, atomic Na was ruled out as an *n*-type dopant to the thiophene materials. In the present case, the contamination is Na^+ instead of Na, so that a doping interaction is even less likely.

B. Electrical response to Na^+ redistribution

These combined observations demonstrate that the organic material is contaminated with mobile Na^+ ions originating from the glass substrate and that it is the electric-field induced redistribution of the ions that causes the gradual changes in electrical properties. We will now discuss how ionic motion can result in electrical changes.

Before the application of a stress bias, the positive charge of the uniformly distributed Na^+ ions is compensated by negative charge (as a whole, the device remains charge neutral). The application of a voltage causes a redistribution of the Na^+ ions inside the organic material. It is unclear how this redistribution affects the compensating charge of the sodium ions. For example, if we consider the case of negative countercharge fixed in the substrate, the redistribution of Na^+ ions results in a change of the electrostatic profile in the organic film and a change of charge-carrier density, similar to what happens in a field-effect transistor under the application of a gate voltage. This is schematically depicted in Fig. 10. Since both the contact and bulk resistances of the organic film are strongly dependent on the carrier density, the ionic redistribution causes large changes in both resistances. We expect similar effects occurring in the cases of negative counterions that are mobile or positive ions (such as H^+) moving in the opposite direction of the sodium motion. In all cases, the electrostatic profile in the organic material will change.

This mechanism explains the sensitivity of the changes to the applied stress bias polarity, their reversibility, and the long times over which they take place: After removing the electric field, the Na^+ ions are attracted by the negative charge in the substrate and by their concentration gradient so

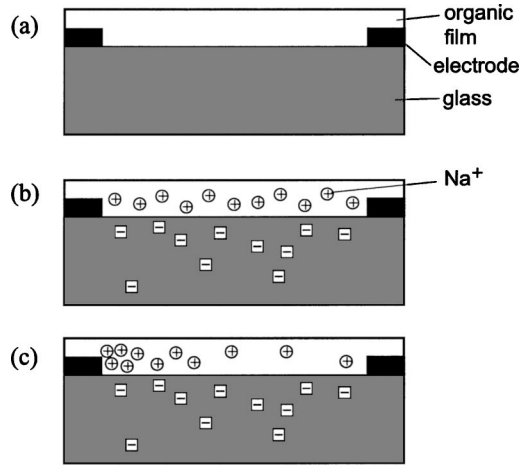

FIG. 10. Schematic picture of the diffusion and redistribution of charged sodium impurities in organic films on alkali-rich glass substrates under the assumption of fixed negative countercharge. Panel (a) shows an as-prepared, undoped device. Sodium contamination is absent in the organic film. At elevated temperatures, however, ionic sodium (Na^+) diffuses into the organic film, leaving negative counterions immobilized in the glass. This is shown in panel (b). Panel (c) shows how the application of electrical stress results in a redistribution of the Na^+ ions toward the cathode.

that they slowly relax to a uniform distribution.

The electrostatic effect of ionic redistribution also explains the similarity between the decrease in activation energy of charge transport with stressing and with increasing hole densities (Fig. 4) since the redistribution is accompanied by an increase in hole density. Finally, the mechanism can account for the observed change in both the bulk and contact resistances: As more Na^+ ions are accumulated close to the cathode, less ions remain in the bulk. Consequently, the negative counter ions induce an increased density of holes in the polymer bulk. At the same time, the accumulation of Na^+ ions at the cathode depletes the electrode of free holes, so that the contact resistance increases while that of anode decreases due to the depletion of Na^+ ions. In devices with a small interelectrode distance, this results in asymmetric $I-V$ characteristics [Fig. 2(b)]. A technique such as scanning Kelvin-probe microscopy could be used to verify the changed contact resistances as well as to map the overall electrostatic effect of the Na^+ motion in detail.[18]

C. Implications for devices

Our measurements show that the choice of glass substrate is crucial to the stability of devices on glass. By choosing a substrate with a negligible concentration of alkali compounds, the device characteristics are much more stable, as shown in Figs. 5 and 8. It should be noted, however, that a small sensitivity to the stressing bias remains, which we attribute to the motion of remnant dopants (for example, due to oxygen) in the organic film under the influence of the electric field.[17] These impurities do not originate from the substrate but have a similar effect on the $I-V$ characteristics: They effectively change the local charge-carrier density, on timescales similar to those discussed for the case of Na^+ redistribution. The motion of dopants in P3HT results in an asymmetry in the $I-V$ characteristics that is opposite to the asymmetry due to Na^+ redistribution. This could be related to the negative charge of the oxygen in the organic material as opposed to the positive charge of the Na^+.

V. SUMMARY AND CONCLUSIONS

In summary, our results demonstrate that the electric-field redistribution of ionic impurities systematically causes hysteresis effects and device instabilities during the operation of organic thin-film devices. Moreover, glass substrates can be a source of such ionic impurities. This was shown for thin films of P3HT and pentacene deposited on glass. Na^+ ions that originate from the glass substrate redistribute inside the organic material under the influence of an electric field. The combined electrostatic effects of mobile ions in the organic film and their counterions result in an increased concentration of holes in the bulk and near one contact, which changes the bulk and contact resistances. Redistribution of ions toward the cathode, therefore, causes the (reversible) emergence with time of asymmetry in the device characteristics. Our results provide a detailed physical picture of the role of mobile impurities in device instabilities, and also imply that the choice of glass with low concentrations of sodium is crucial for device applications as well as fundamental studies of the electrical characteristics of organic films deposited on glass. The similarity of the effects for P3HT and pentacene—prototypical examples of organic semiconducting polymers and oligomers, respectively— demonstrates that our conclusions are relevant for a wide range of organic materials.

ACKNOWLEDGMENTS

This work was part of the research program of the ''Stichting voor Fundamenteel Onderzoek der Materie (FOM),'' which was financially supported by the ''Nederlandse Organisatie voor Wetenschappelijk Onderzoek (NWO).'' One of the authors (A.F.M.) gratefully acknowledges support from the NWO Vernieuwingsimpuls. The authors thank B. H. Huisman for his advice and for synthesizing the P3HT. They also acknowledge E. J. Meijer for bringing the issue of glass to their attention as well as for supplying substrates.

[1] For two recent overviews of the field of organic electronics, see D. Voss, Nature (London) **407**, 442 (2000); J. M. Shaw and P.F. Seidler, IBM J. Res. Dev. **45**, 3 (2001).
[2] A.R. Brown, C.P. Jarrett, D.M. de Leeuw, and M. Matters, Synth. Met. **88**, 37 (1997).
[3] W.A. Schoonveld, J.B. Oostinga, J. Vrijmoeth, and T.M. Klapwijk, Synth. Met. **101**, 608 (1999).
[4] M. Matters, D.M. de Leeuw, P.T. Herwig, and A.R. Brown, Synth. Met. **102**, 998 (1999).
[5] S.J. Zilker, C. Detcheverry, E. Cantatore, and D.M. de Leeuw, Appl. Phys. Lett. **79**, 1124 (2001).
[6] G. Horowitz, R. Hajloui, D. Fichou, and A. Kassmi, J. Appl. Phys. **85**, 3202 (1999).
[7] S. Scheinert, G. Paasch, S. Pohlmann, H.-H. Hörhold, and R. Stockmann, Solid-State Electron. **44**, 845 (2000).
[8] Z.D. Popovic and H. Aziz, IEEE J. Sel. Top. Quantum Electron. **8**, 362 (2002).
[9] P.E. Burrows, V. Bulovic, S.R. Forrest, L.S. Sapochak, D.M. McCarty, and M.E. Thompson, Appl. Phys. Lett. **65**, 2922 (1994).
[10] H. Sirringhaus, P.J. Brown, R.H. Friend, M.M. Nielsen, K. Bechgaard,

B.M.W. Langeveld-Voss, A.J.H. Spiering, R.A.J. Janssen, E.W. Meijer, P. Herwig, and D.M. de Leeuw, Nature (London) **401**, 685 (1999).
[11] Y.-Y. Lin, D.J. Gundlach, S.F. Nelson, and T.N. Jackson, IEEE Electron Device Lett. **18**, 606 (1997).
[12] R.D. McCullough, R.D. Lowe, M. Jayaraman, and D.L. Anderson, J. Org. Chem. **58**, 904 (1993).
[13] D.B.A. Rep, B.-H. Huisman, E.J. Meijer, P. Prins, and T.M. Klapwijk, Mater. Res. Soc. Symp. Proc. **660**, JJ 7.9.1 (2001).
[14] M.S.A. Abdou, F.P. Orfino, Y. Son, and S. Holdcroft, J. Am. Chem. Soc. **119**, 4518 (1997).
[15] American Society for Testing and Materials, Surf. Interface Anal. **17**, 889 (1991).
[16] C.D. Wagner, L.E. Davies, M.V. Zeller, J.A. Taylor, R.M. Raymond, and L.H. Gale, Surf. Interface Anal. **3**, 211 (1981).
[17] D.B.A. Rep, A.F. Morpurgo, and T.M. Klapwijk (unpublished).
[18] L. Bürgi, H. Sirringhaus, and R.H. Friend, Appl. Phys. Lett. **80**, 2913 (2002).
[19] We have studied dopant redistribution effects in alkali-free devices highly doped with iodine or oxygen, and found that they did not show asymmetric characteristics after stressing. Instead, a rapid, small, and symmetric increase in current during stressing followed by a slow decrease was observed. We attribute the current increase to heating effects, since the doped devices are operated at a high current density. The subsequent decrease is due to the slow outdiffusion of dopants. The absence of asymmetry in the device characteristics (due to the fact that the contact resistances decrease with doping) makes it impossible to observe redistribution effects using the method described here.
[20] For this calculation, we define a ''unit cell'' containing one thiophene ring and one hexyl chain, of size 0.38 nm $\times$ 0.38 nm $\times$ 1.64 nm. These numbers were taken from x-ray diffraction measurements done in our lab, as well as data taken from literature.
[21] It can be seen in Fig. 9 that the carbon-to-sulphur ratio is about 18, which is larger than the number of 10 expected from the chemical formula. A difference in angle dependence of the XPS signal for carbon and sulphur might be the cause of this discrepancy.
[22] G. Moretti, J. Electron Spectrosc. Relat. Phenom. **95**, 95 (1998).
[23] Reference data were taken from the National Institute for Standards and Technology X-ray Photoelectron Spectroscopy Database, http://srdata.nist.gov/xps/
[24] An overview of reports on alkali migration from glass substrates is given by N. Janke, O. Grassmé, and R. Weißman, Glass Sci. Technol. (Frankfurt/Main) **73**, 143 (2000).
[25] E.H. Snow, A.S. Grove, B.E. Deal, and C.T. Sah, J. Appl. Phys. **36**, 1664 (1965).
[26] J. Murr and C. Ziegler, Phys. Rev. B **57**, 7299 (1998).
[27] R.P. Mikalo and D. Schmeißer, Synth. Met. **127**, 273 (2002).